



A numerical model to evaluate the effect of hydrogen embrittlement on low-alloy steels

L. Vergani, G. Gobbi, C. Colombo

Department of Mechanical Engineering, Politecnico di Milano, Milano (Italy)

laura.vergani@polimi.it, giorgia.gobbi@polimi.it, chiara.colombo@polimi.it

ABSTRACT. Some extreme working environments are characterised by corrosive conditions, able to develop hydrogen formation. The presence of atomic hydrogen localized in correspondence of plastic strains at the crack tip modifies the steel behaviour and its macroscopical mechanical properties. The phenomenon of hydrogen embrittlement is, indeed, one of the main responsible for the increase in fatigue crack growth rate and life reduction. For this reason, it is important to have validated numerical models able to estimate the mechanical behaviour of material in presence of hydrogen. Aim of this study is to develop a numerical model of two low-alloyed steels used in pipelines applications. Numerical simulations of C(T) specimens are carried out in different steps, considering hydrogen presence/absence combined with local plastic strains of the material. These two parameters are, indeed, responsible for a drop in material toughness, therefore for an increased crack growth rate. Two modelling techniques are used to simulate crack propagation: application of cohesive elements characterised by laws of degradation of mechanical properties, and the virtual crack closure technique (VCCT). Once model is validated by a comparison with experimental toughness measures, final considerations on the most valid simulation technique for the considered case are proposed.

SOMMARIO. Alcuni ambienti estremi di lavoro sono caratterizzati da fenomeni corrosivi che sviluppano la formazione di idrogeno. La presenza di idrogeno atomico localizzato in corrispondenza delle deformazioni plastiche all'apice della cricca modifica macroscopicamente il comportamento dell'acciaio e le sue proprietà meccaniche. Il fenomeno dell'infragilimento da idrogeno è, infatti, uno dei principali responsabili dell'aumento nella velocità di propagazione delle cricche e della riduzione della vita a fatica. È quindi importante avere a disposizione dei modelli numerici convalidati, che permettano di stimare il comportamento meccanico dei materiali in presenza di idrogeno. Scopo di questo studio è lo sviluppo e la validazione di un modello numerico di due acciai bassoalegati utilizzati per oleodotti. Sono state condotte, simulazioni numeriche su provini C(T) in diversi *step* considerando o meno la presenza di idrogeno combinata con le deformazioni plastiche nel materiale. Questi due parametri sono, infatti, responsabili della perdita di tenacità del materiale, e dunque dell'aumento della velocità di propagazione delle cricche. Due tecniche di modellazione sono utilizzate per simulare la propagazione della cricca: l'applicazione di elementi coesivi caratterizzati da leggi di degrado delle proprietà meccaniche, e la *virtual crack closure technique* (VCCT). Una volta convalidato il modello dal confronto con le misure sperimentali di tenacità, si propongono delle considerazioni finali sulla tecnica di simulazione più valida per il caso in esame.

KEYWORDS. Hydrogen embrittlement; Fracture toughness; Numerical simulation; Virtual crack closure technique



INTRODUCTION

Applications of carbon and low alloy steels in environments characterized by the presence of hydrogen are frequently subjected to the well-known phenomenon of hydrogen embrittlement. Atomic hydrogen diffuses in the steel lattice and its macroscopical effects are related to the degradation of mechanical properties, as fracture toughness, and fatigue performances of the material. Embrittlement of mechanical behaviour of steel is a complex mechanism, not fully understood; some mechanisms have been proposed in the literature, with the aim of explaining the interaction of atomic hydrogen with steel lattice, thus starting from the atomistic scale, to clarify the resulted decrease in mechanical properties.

Influence of hydrogen is deeply dependent on material microstructure: indeed, atomic hydrogen into a metal can diffuse through normal interstitial lattice sites (NILS). In regions characterized by tensile hydrostatic stress and soften elastic modulus, hydrogen has a low chemical potential; gradients in this potential activate motion of the small hydrogen atoms [1]. During this motion, hydrogen is trapped in specific sites, which are related to the material microstructure. The trap sites for atomic hydrogen can be reversible or irreversible. Examples of the first type are dislocations, related to the presence of plastic strain in the steel, grain boundaries and interfaces, vacancies and cavities [2,3]. The second ones, on the contrary, are oxides, sulfides and carbides of titanium, niobium or vanadium, which are very dangerous since hydrogen atoms are irreversibly localized and locked. The contribution of trap sites is quantitatively the most relevant on hydrogen embrittlement phenomenon. For this reason, many studies in the literature focus on the investigation of the trap sites in terms of density, binding energy and their correlation with the stress state of the material.

Different hydrogen diffusion models considering the influence of trapping sites were developed. Most of these are based on McNabb and Foster [4] formulation neglecting the interaction between hydrogen concentration and plastic strain. Instead, Sofronis and McMeeking [5] described a hydrogen diffusion model considering the effect of hydrostatic stress and trapping due to plastic strain, focusing the attention on the region around a blunting crack tip. They established a correlation between the number of traps and the plastic strains that seem to mainly affect the total hydrogen concentration rather than the hydrostatic stress.

Various mechanisms for hydrogen embrittlement have been proposed in past; one of the most accepted is the hydrogen enhanced localized plasticity (HELP) mechanism [6]. It is based on observations that hydrogen decreases barriers to dislocation motion: during fatigue tests in presence of hydrogen, slip bands localize near the crack tip. Indeed, hydrogen is strongly locked to defects, and in particular it concentrates at crack tips, where plastic strains are generated by stress intensification. Its presence increases crack growth rate and, therefore, deeply modifies residual fatigue life of the component. Together with this effect, hydrogen embrittlement also causes loss in mechanical ductility, toughness reduction, degradation of fatigue properties and changes in metallic bonding [7].

In the design stage and for a proper maintenance of mechanical and structural applications, as fuel cells, vessels for hydrogen storage or pipelines for hydrocarbons, knowledge of validated models to understand fatigue crack growth and fracture toughness is a basic tool for engineers. In the literature, some experimental data and analytical models are available. Most of these papers are dedicated to austenitic and stainless steels [8,9], but some also deal with carbon high-strength low-carbon steels [10], which are, however, commonly used in many applications, where hydrogen presence cannot be neglected.

Experimental results used in this paper for validation of numerical simulations come from a previous study [11] on two steels, whose typical application is for pipeline: a low alloy steel, 2 1/4 Cr 1 Mo - ASTM A182 (namely F22) and a micro-alloyed C-Mn steel -API 5L (namely X65). In the following paragraphs, a description of a numerical model creation and simulations performed to describe hydrogen influence on fracture toughness tests are described. Two modelling techniques are used to simulate crack propagation: the application of cohesive elements characterised by laws of degradation of mechanical properties near to failure, and the virtual crack closure technique VCCT. After the validation of the models, discussion on the used techniques is proposed in order to define the best solution to reproduce the toughness behaviour of steels in presence of hydrogen.

EXPERIMENTAL TESTS

In this paragraph a brief recall on results obtained from experimental toughness tests is presented [11]. Two pipes in F22 and X65 steels were considered and C(T) specimens were extracted along longitudinal direction (C-L orientation, in accordance to ASTM E1823). These specimens are characterized by a width $W = 40$ mm; the geometry is in

accordance with ASTM 647 standard (Fig. 1). Thickness of the specimens is set to 20 mm. Tests were carried out considering specimens “as received”, thus without hydrogen, or after a hydrogen charge. The experimental procedure of hydrogen charging was performed as described in [12]: this electrochemical procedure allows having a final hydrogen concentration till a maximum value of 2 ppm. Measures of hydrogen presence were performed on different specimens and the values of hydrogen concentration resulted repeatable. ASTM 1820 standard was followed to perform fracture toughness tests. Between hydrogen charge and effective test procedure, specimens are maintained in liquid nitrogen in order to avoid hydrogen loss and to keep constant its concentration.

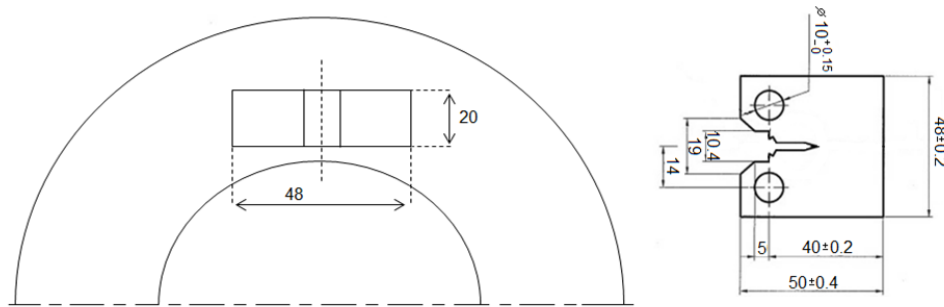


Figure 1: Specimen extraction from the pipe and geometry (mm)

NUMERICAL MODEL

A finite element model, consisting of three sequential steps of simulations, is developed using the numerical software Abaqus 6.11-2. The three steps of analysis include: an elastic-plastic stress analysis on uncharged material, a mass diffusion analysis influenced by the stress state previously calculated and a last elastic-plastic stress analysis with hydrogen influence, affecting the crack propagation behaviour, simulated by two different techniques. These are cohesive elements application and virtual crack closure technique (VCCT).

A bi-dimensional C(T) specimen is modelled reproducing the dimensions of the specimens considered in the experimental tests (Fig. 1). Two geometries are developed according to the requirements of the crack propagation technique adopted for the third step of the simulation. Therefore, using cohesive elements a schematization of only half part of the specimen is possible, exploiting the symmetry with respect to the horizontal axis, while the VCCT technique requires the whole specimen. It is composed by two symmetric half parts combined along the crack propagation plane.

The same mesh is maintained over all the three steps of simulation in order to correlate the output of a simulation to the input of the next one. The minimum element dimensions along the crack propagation plane are chosen after an optimization process, focused on obtaining an element size able to guarantee a good resolution of strain and stress at the crack tip. The dimensions, defined by this optimization process, are 10 μm for the model implementing the cohesive elements and 30 μm for that including the VCCT technique. The elements are 4 nodes linear plane strain type for the stress analyses and 4 nodes linear mass diffusion type for the diffusion analyses.

First step - Elastic-plastic stress analysis

The first step of the model consists of an elastic-plastic stress analysis without hydrogen presence. The material properties are defined on the base of the experimental tensile tests results shown in Fig. 2. Regard to the elastic properties of the material, Young’s modulus and Poisson’s ratio values are assigned to each one of two steels as reported in tab. 1. Plastic component of the material properties, instead, has been defined providing the entire strain-stress curve removing the elastic part from the total strain.

Material	E [MPa]	σ_Y [MPa]	ν
SA-182 F22	206500	468	0.3
API 5L X65	206200	511	0.3

Table 1: Mechanical properties of the analysed steels, according to [11].

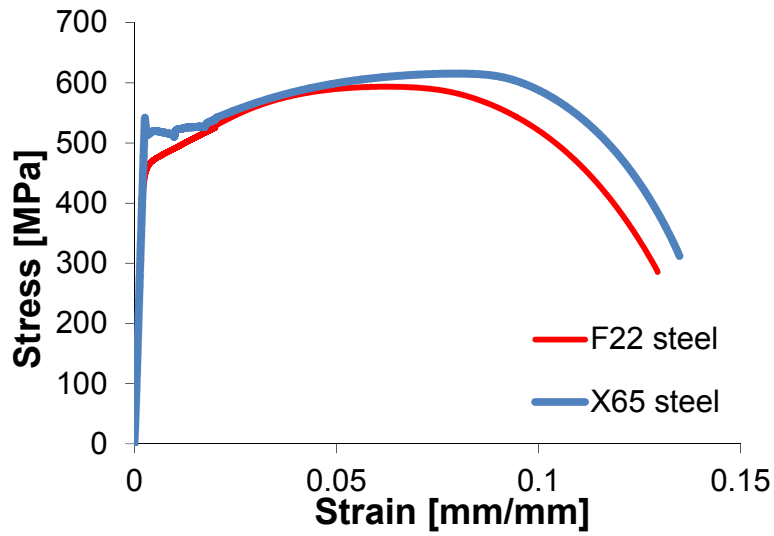


Figure 1: Stress-strain curves of F22 and X65 steels

Second step – Mass diffusion analysis

The second step consists of a diffusion analysis. It starts from a fixed initial hydrogen concentration equal to 1.5 ppm constant in the specimen and on the base of the hydrostatic stress, evaluated in the previous step of analysis, the redistribution of the hydrogen is estimated. Mass diffusion analysis is a transient type analysis in which the time is defined in order of 10 min. It corresponds to the time required to reach the maximum load value during the experimental tests, carried out to determine the toughness. The stress state imported by the previous simulation step remains constant during the diffusion analysis. The governing equations for mass diffusion are an extension of Fick's model [13]:

$$\frac{\partial C}{\partial t} = D \nabla^2 C + D \frac{\bar{V}_H}{R(T - T^z)} \nabla C \cdot \nabla p + D \frac{\bar{V}_H}{R(T - T^z)} C \nabla^2 p \quad (1)$$

where C is the hydrogen concentration, D is the diffusion coefficient, $\bar{V}_H = 2.0 \cdot 10^3 [\text{mm}^3 / \text{mol}]$ is the partial molar volume of hydrogen for iron alloy [14], $R = 8.31 [\text{J} / \text{molK}]$ is the gas constant, T is the temperature and T^z the absolute zero temperature and p is the hydrostatic stress. The diffusion coefficients for the two steels are set as $D_{F22} = 1.75 \cdot 10^{-11} [\text{m}^2 / \text{s}]$ and $D_{X65} = 2 \cdot 10^{-10} [\text{m}^2 / \text{s}]$ according to experimental tests carried out by [15]. Mass diffusion analysis allows determining only the hydrogen concentration related to the interstitial lattice sites, NILS.

Third step – Cohesive elements

Considering the application of cohesive elements during this last step of the analysis, half the specimen is considered. On the symmetry plane cohesive elements with infinitesimal thickness are placed. They are tied on the upper side to the elements simulating the steel specimen, while, on the lower side, boundary conditions of symmetry are applied. Using this technique the fracture occurs at the interface of cohesive elements incorporated into the model in the third step of analysis. Therefore, no continuum element is damaged using cohesive model. There is only a relative displacement of the upper face with respect to the bottom one that represents the crack opening. In fact, the behaviour of the material in the cohesive zone is regulated by a traction separation law (TSL), in which the cohesive stress (σ) is function of traction separation (δ). The area below the curve in σ - δ diagram represents the cohesive energy Γ_C . Different shapes of TSL curve are possible, linear or polynomial are proposed in [13]. The possibility to change the shape of the TSL curve according to the type of the problem is one of the main features and definitively an advantage of this technique.

The definition of the cohesive elements and their traction separation law are implemented in the model using a UEL subroutine (user-defined element), which allows the user to define the properties of an element, and available in Abaqus software. Starting from a UEL subroutine available in the literature for a potential based traction separation law [16], this was adapted for the present problem. A new traction separation law with a trapezoidal shape has been considered (Fig. 3 blue curve), modelled in order to ensure the convergence of the analysis. Five parameters are required into the subroutine



to outline the geometry of the curve: $Tn1$, $\delta1$, $Tn2$, $\delta2$, δn . Moreover, for each increment of the simulation the maximum normal separation value in correspondence of the integration points is registered as state variable. An algorithm implemented into the UEL subroutine compares, increment by increment, the current value of the normal separation with the maximum value recorded in the previous increment. For each time increment, the software evaluates if the element is more damaged and therefore it increases crack opening, or if the element can be elastically unloaded and reloaded (Fig. 3 green curve).

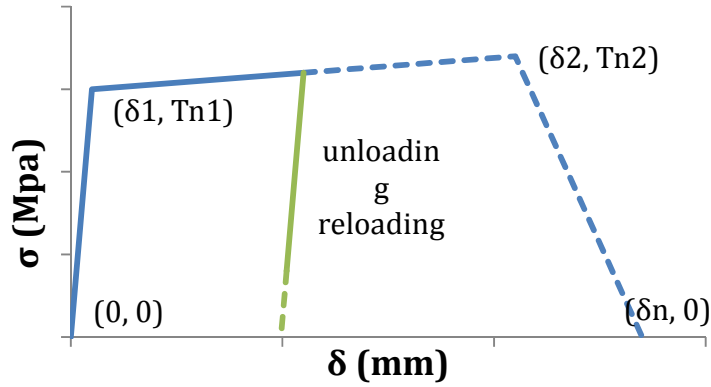


Figure 2: Traction separation law implemented for cohesive elements

The hydrogen concentration field calculated by the previous step is transferred to the third step, importing it as initial condition of the analysis. As already mentioned, it corresponds to the interstitial lattice sites hydrogen concentration. However, it is known that the trap sites have a significant role in hydrogen embrittlement phenomenon.

Therefore, in order to consider the presence of reversible traps on hydrogen diffusion, it is necessary to implement in the model an additional equation that allows correlating the hydrogen concentration with the plastic strain. Based on the results of Sofronis and Taha [3] on high and low-strength steels a linear correlation between trapped hydrogen concentration and plastic strain is proposed by [17]:

$$C_T = (49.0\varepsilon_p + 0.1C_L) \quad (2)$$

where C_T is the hydrogen concentration in traps, ε_p is the plastic strain and C_L is the diffusible hydrogen concentration calculated by Eq.1. This relation is applied in the third step. Therefore, the total hydrogen concentration considered in the last step is the sum of C_T and C_L hydrogen amount. The total concentration is used to reduce the material properties into the cohesive zone, simulating the hydrogen embrittlement effect. On the base of [18], the hydrogen influence is taken into account decreasing the cohesive energy Γ_c proportionally to the hydrogen coverage \mathcal{G} [14]:

$$\frac{\Gamma_c(\theta)}{\Gamma_c} = 1 - 1.0467\theta + 0.1687\theta^2 \quad (3)$$

The hydrogen coverage is defined as function of hydrogen concentration C and the difference of Gibbs free energy between the interface and surrounding material [19]:

$$\mathcal{G} = \frac{C}{C + \exp(-\Delta g_b^0 / RT)} \quad (4)$$

The difference of Gibbs free body Δg_b^0 is considered equal to 30 kJ/mol [14].

Therefore, it is possible to establish the decreasing factor of the cohesive energy but the new shape of the TSL curve is unknown. It is needed to find the most appropriate shape validating the experimental results.

Third step – Virtual crack closure technique

The virtual crack closure technique (VCCT) has been developed as an alternative to the application of cohesive elements to the numerical model; it requires the definition of a master and slave surfaces between which the crack propagates. When crack propagates there is not only a displacement between two faces, like it happens for cohesive elements, but the

nodes of the elements in contact on the crack surface are opened. In fact, the VCCT method is based on the definition of the energy release rate value G [20]. From opening displacements of the crack surfaces, equivalent strain energy release rate G_{equiv} is estimated in the crack region; to determine whether an element fails or not, this value is compared to a critical value G_{equivC} . This critical value of the energy is obtained starting from the critical value in the configuration without hydrogen, and it is multiplied by a reducing factor.

The critical value of energy, G_{equivC} , without hydrogen, is computed by Abaqus using BK (Benzeggagh and Kenane) law [13] starting from experimental measures of J . The reducing coefficient, used to evaluate hydrogen embrittlement influence, is estimated using two different subroutines: URDFIL (User subroutine to read the results file) and UFIELD (User subroutine to specify predefined field variables). The first one is recalled at the beginning of every new increment to read for each nodes of the model the values of the equivalent plastic strain and the hydrogen concentration imported from the previous analyses. These values are stored in order to make them available to all other Abaqus subroutines. The UFIELD subroutine uses the two variables previously mentioned and combines them on the base of Eq. 2 to obtain the reducing factor of the material properties in presence of hydrogen. When G_{equiv} is equal to G_{equivC} , the nodes on the crack front are released.

RESULTS AND DISCUSSION

The model is developed in three sequential steps. The first two steps are unique and the results show a similar trend for the considered steels. From the first step, the stress state on hydrogen uncharged material is detected and it is provided to the second step. Fig. 4 reports the hydrostatic stress contour related to F22 steel as example.

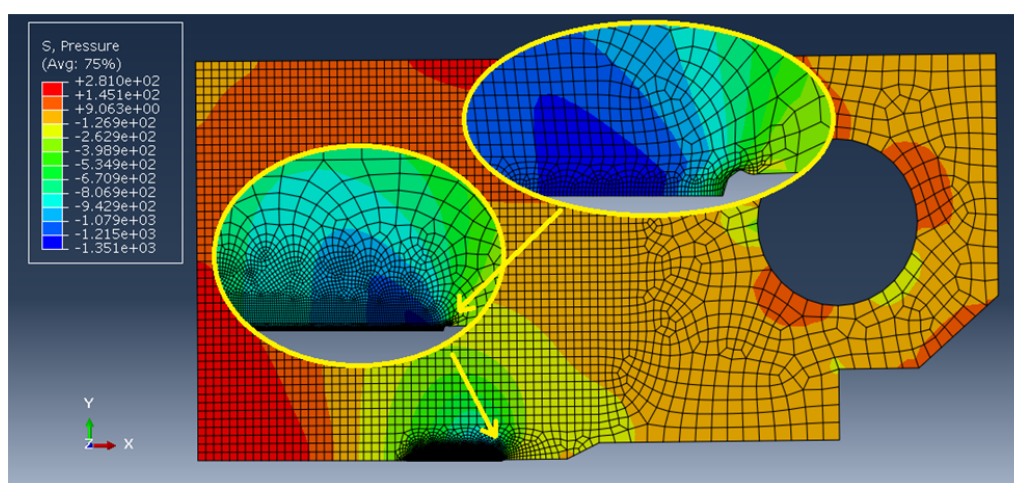


Figure 3: Hydrostatic stress contour related to F22 steel, from step 1.

ue of the interstitial hydrogen concentration, associated to the hrostatic sess previously evaluated, is determined during the second step othe analysis. Different results are associated with the two different tiques implemented into the model in the last step of analysis. Figure 5 shows the vertical stress field, S22, related to the cohesive elements model (Fig. 5a) and the equivalent plastic strain field concerning the VCCT technique (Fig. 5b).

Observing the S22 stress trend that corresponds to the traction stress of the TSL cohesive elements law, it is visible that where the stress is equal to zero (green zone on the propagation plane) the normal separation exceeded the limit δn and the crack is propagated. From the same figure it appears evident also the main limit of the cohesive elements approach. Although it is a technique able to estimate the crack propagation, the traction separation law requires a very large displacement. Consequently, there is not a concentration of the maximum stress at the crack tip but a redistribution of the stress occurs over a wider area (red zone). This technique results inadequate to appreciate the plastic strains accumulated at the crack front. It is the most important aspect to evaluate the hydrogen trap concentration and correlate this with the degradation of the material properties.

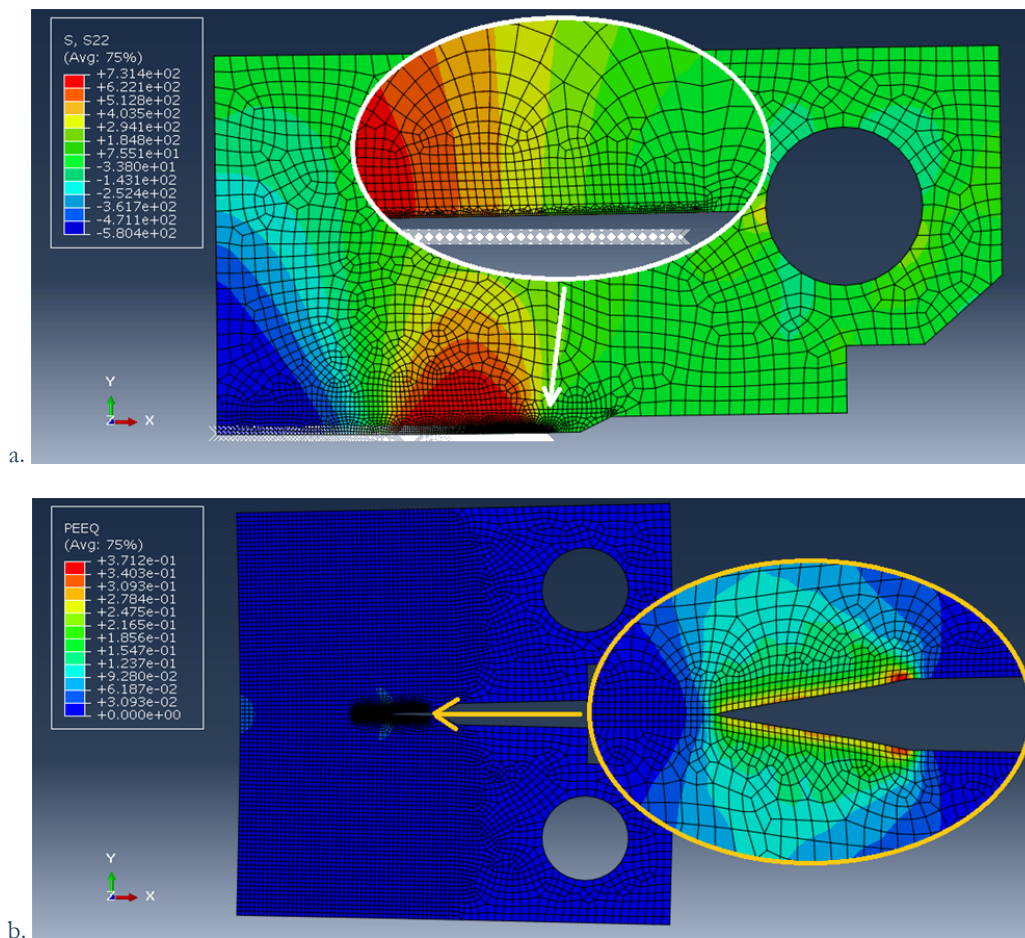


Figure 5: Step 3: a. Stress field along vertical direction, with cohesive elements application; b. equivalent plastic strain field, with VCCT

In regards to the results obtained by VCCT technique, Fig. 5 represents the plastic strain intensification in front of the crack. It is also visible the crack opening and the plastic wake around the crack during its propagation. This makes the VCCT analysis more accurate in order to estimate the trap sites correlate to the plastic strains. For this reason, the selected technique to validate the model, by a comparison with experimental tests data, is the VCCT technique. The cohesive element model, instead, was neglected because of its limits to reproduce the behaviour of the steels when crack propagates.

During the third step, the value of G_{equivC} , estimated in function of the total hydrogen concentration, is calculated by the numerical simulation. Fig. 6 shows the G_{equivC} values trend in the specimen related to F22 steel as example. Value of G_{equivC} in correspondence of crack tip can be compared with the experimental J values obtained by tests on hydrogen charged materials in order to validate the model. Tab. 2 summarizes the experimental and numerical values.

From the numerical simulation on X65 steel, the values of J associated to the embrittlement effect of hydrogen reflect the experimental values, and the difference between these two values of energy is extremely low.

On the contrary, for F22 steel, the numerical solution underestimates J value for hydrogen charged material. This discrepancy is probably due to the fact that the experimental J_{IC} value for uncharged material is a minimum value and probably the correct real toughness is higher.

Results of numerical simulations are therefore in good accordance with experimental tests for X65, while for F22 steel differences are evident, even if a huge drop in J value, thus embrittlement effect of hydrogen, can clearly be appreciated.

Although this numerical model can still be improved, this is surely a first approach which can be optimized and extended to the study of hydrogen embrittlement phenomenon in other materials or in more complex structures.

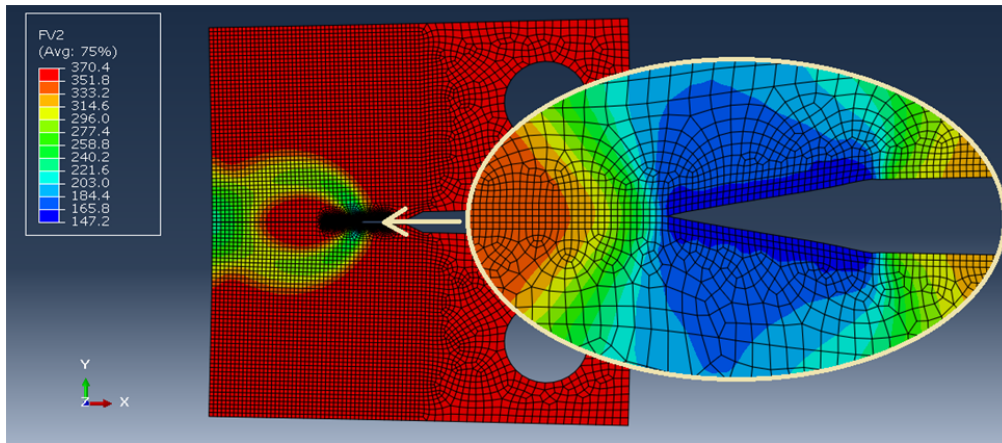


Figure 6: Evaluation of G_{equivC} by VCCT

Material	J uncharged material	J charged material	
	[N/mm]	[N/mm]	Numerical value [N/mm]
82 F22	>941.6	211.0	147.3
API 5L X65	>922.0	146.7	152.3

Table 2: Experimental and numerical toughness values for charged and uncharged X65 and F22 steels.

CONCLUSIONS

From numerical simulations carried out in this paper it is possible to draw some conclusions. A numerical model of a C(T) specimen in presence of atomic hydrogen is carried out: the simulation consists in an over-imposition of an elastic-plastic stress analysis and a diffusion analysis. These two steps are then combined in a third analysis, where crack propagation is performed.

Two numerical techniques for crack propagation are taken into account, based on cohesive elements and virtual crack closure technique (VCCT) methods. These techniques include a formulation to define degradation of material properties in presence of hydrogen, located in interstitial lattice sites and reversible traps. Both cohesive element application and VCCT method are valid for the present case, but VCCT results the most easily implementable in the considered finite element software. Moreover, VCCT allows a more correct evaluation of plastic strain at the crack tip and its flow along crack propagation.

From comparison with experimental data collected in absence and presence of hydrogen, a validation of the model is proposed; results of numerical simulations are in good accordance with experimental tests for one of the tested material, while for the second steel differences are evident, even if a huge drop in mechanical properties, thus embrittlement effect of hydrogen, can be clearly appreciated.

Although this numerical model can still be improved, this is surely a first attempt which can be optimized and extended to the study of hydrogen embrittlement phenomenon in other materials or in more complex structures.

REFERENCES

- [1] P. Sofronis, *J. Mech. Phys Solids*, 43 (1995) 1385.
- [2] A.J. Kumnick, H.H. Johnson, *Acta Metallurgica*, 28 (1980) 33.
- [3] A. Taha, P. Sofronis, *Eng. Fract. Mech.*, 68 (2001) 803.
- [4] A. McNabb, P.K. Foster, *Trans. Metall. Soc. AIME*, 33 (1996) 1709.
- [5] P. Sofronis, R.M. McMeeking, *J. Mech. Phys. Solids*, 37 (1989) 317.



- [6] H. K. Birnbaum, P. Sofronis, *Mater. Sci. Engng.*, A176 (1994) 191.
- [7] RP. Gangloff, in: *Comprehensive Structural Integrity*, Edited by I. Milne, R.O. Ritchie and B. Karahaloo, Elsevier Science, USA, (2003) 31.
- [8] Y. Murakami, T. Kanezaki, Y. Mine, S. Matsuoka, *Met. Mater. Trans.*, A39 (2008) 1327.
- [9] T. Kanezaki, C. Narazaki, Y. Mine, S. Matsuoka, Y. Murakami, *Int. J. Hydrogen Energy*, 33 (2008) 2604.
- [10] Y. Murakami, S. Matsuoka, *Eng. Fract. Mech.*, 77 (2010) 1926.
- [11] P. Fassina, F. Bolzoni, G. Fumagalli, L. Lazzari, L. Vergani, A. Sciuccati, *Eng. Fract. Mech.*, 81 (2012) 43.
- [12] E. Fallahmohammadi, F. Bolzoni, L. Lazzari, *Int. J. Hydrogen Energy*, 38 (2013) 2531.
- [13] Abaqus v.6.12 documentation, Dassault Systèmes Simulia Corp.
- [14] S. Serebrinsky, E. A. Carter, M. Ortiz, *J. Mech. Phys. Solid*, 52 (2004) 2403.
- [15] F. Bolzoni, P. Fassina, G. Fumagalli, L. Lazzari, *G. Re Proceedings of the European Corrosion Congress EUROCORR*, Moscow, September 2010
- [16] K. Park, G. H. Paulino, *Eng Fract Mech*, 93 (2012) 239.
- [17] V. Olden, C. Thaulow, R. Johnsen, E. Ostby, T. Berstad, *Eng Fract Mech*, 76 (2009) 827.
- [18] V. Olden, A. Alvaro, O.M. Akselsen: *Int. J. Hydrogen Energy*, 37 (2012) 11474.
- [19] E. D. Hondros, M.P. Seah, *Metall Trans*, 8 (1977) 1363.
- [20] R. Krueger, *Appl. Mech. Rev.*, 57 (2004) 109.